Optofluidic lab-on-a-chip for rapid algae population screening

Allison Schaap,[1] Yves Bellouard,[1,*] and Thomas Rohrlack[2]

[1]*Mechanical Engineering Department, Eindhoven University of Technology, Eindhoven, The Netherlands*
[2]*Norwegian Institute for Water Research, Gaustadalléen 21, 0349 Oslo, Norway*
*y.bellouard@tue.nl

Abstract: The rapid identification of algae species is not only of practical importance when monitoring unwanted adverse effects such as eutrophication, but also when assessing the water quality of watersheds. Here, we demonstrate a lab-on-a-chip that functions as a compact robust tool for the fast screening, real-time monitoring, and initial classification of algae. The water-algae sample, flowing in a microfluidic channel, is side-illuminated by an integrated subsurface waveguide. The waveguide is curved to improve the device sensitivity. The changes in the transmitted optical signal are monitored using a quadrant-cell photo-detector. The signal-wavelets from the different quadrants are used to qualitatively distinguish different families of algae. The channel and waveguide are fabricated out of a monolithic fused-silica substrate using a femtosecond laser-writing process combined with chemical etching. This proof-of-concept device paves the way for more elaborate femtosecond laser-based optofluidic micro-instruments incorporating waveguide networks designed for the real-time field analysis of cells and microorganisms.

©2011 Optical Society of America

OCIS codes: (130.3990) Micro-optical devices; (130.6010) Sensors; (130.2755) Glass waveguides; (130.3120) Integrated optics devices; (280.1415) Biological sensing and sensors

References and Links

1. E. M. Jochimsen, W. W. Carmichael, J. S. An, D. M. Cardo, S. T. Cookson, C. E. M. Holmes, M. B. Antunes, D. A. de Melo Filho, T. M. Lyra, V. S. Barreto, S. M. F. O. Azevedo, and W. R. Jarvis, "Liver failure and death after exposure to microcystins at a hemodialysis center in Brazil," N. Engl. J. Med. **338**(13), 873–878 (1998).
2. L. Zhou, H. Yu, and K. Chen, "Relationship between microcystin in drinking water and colorectal cancer," Biomed. Environ. Sci. **15**(2), 166–171 (2002).
3. I. Chorus, and J. Bartram, *Toxic cyanobacteria in water: a guide to their public health consequences, monitoring and management*, (World Health Organization, 1999).
4. European Parliament, "Directive 2006/7/EC of the European Parliament and of the Council of 15 February 2006 concerning the management of bathing water quality and repealing Directive 76/160/EEC," Off. J. Eur. Union **49**, 37 (2006).
5. J. Mouawad, "Exxon to Invest Millions to Make Fuel from Algae," *The New York Times*, New York ed. July 13, 2009, p. B1.
6. D. Schneider, "Bioengineering Algae for Fuels," IEEE Spectrum, July 22, 2009, http://spectrum.ieee.org/energywise/energy/renewables/bioengineering-algae-for-fuels.
7. K. M. Davis, K. Miura, N. Sugimoto, and K. Hirao, "Writing waveguides in glass with a femtosecond laser," Opt. Lett. **21**(21), 1729–1731 (1996).
8. A. Marcinkevičius, S. Juodkazis, M. Watanabe, M. Miwa, S. Matsuo, H. Misawa, and J. Nishii, "Femtosecond laser-assisted three-dimensional microfabrication in silica," Opt. Lett. **26**(5), 277–279 (2001).
9. Y. Bellouard, A. Said, M. Dugan, and P. Bado, "Fabrication of high-aspect ratio, micro-fluidic channels and tunnels using femtosecond laser pulses and chemical etching," Opt. Express **12**(10), 2120–2129 (2004).
10. Y. Bellouard, A. Said, and P. Bado, "Integrating optics and micro-mechanics in a single substrate: a step toward monolithic integration in fused silica," Opt. Express **13**(17), 6635–6644 (2005).
11. Y. Hanada, K. Sugioka, H. Kawano, I. S. Ishikawa, A. Miyawaki, and K. Midorikawa, "Nano-aquarium for dynamic observation of living cells fabricated by femtosecond laser direct writing of photostructurable glass," Biomed. Microdevices **10**(3), 403–410 (2008).
12. Y. Bellouard, A. A. Said, M. Dugan, and P. Bado, "Monolithic three-dimensional integration of micro-fluidic channels and optical waveguides in fused silica," in *Proceedings of Materials Research Society Fall Meeting Symposium A,* Vol. 782 (Materials Research Society, 2003), pp. 63–68

13. A. A. Said, M. Dugan, P. Bado, Y. Bellouard, A. Scott, and J. Mabesa, "Manufacturing by laser direct-write of three-dimensional devices containing optical and microfluidic networks," in Proc. SPIE **5339** (2004).
14. R. W. Applegate, Jr., J. Squier, T. Vestad, J. Oakey, D. W. M. Marr, P. Bado, M. A. Dugan, and A. A. Said, "Microfluidic sorting system based on optical waveguide integration and diode laser bar trapping," Lab Chip **6**(3), 422–426 (2006).
15. R. M. Vazquez, R. Osellame, D. Nolli, C. Dongre, H. van den Vlekkert, R. Ramponi, M. Pollnau, and G. Cerullo, "Integration of femtosecond laser written optical waveguides in a lab-on-a-chip," Lab Chip **9**(1), 91–96 (2009).
16. M. Kim, D. J. Hwang, H. Jeon, K. Hiromatsu, and C. P. Grigoropoulos, "Single cell detection using a glass-based optofluidic device fabricated by femtosecond laser pulses," Lab Chip **9**(2), 311–318 (2009).
17. V. Maselli, J. R. Grenier, S. Ho, and P. R. Herman, "Femtosecond laser written optofluidic sensor: Bragg Grating Waveguide evanescent probing of microfluidic channel," Opt. Express **17**(14), 11719–11729 (2009).
18. V. Pahilwani, Y. Bellouard, A. A. Said, M. Dugan, and P. Bado, "In-situ optical detection of mesoscale components in glass microfluidic channel with monolithic waveguide," Proc. SPIE **6715** (2007)
19. Y. Bellouard, V. K. Pahilwani, T. Rohrlack, A. A. Said, M. Dugan, and P. Bado, "Towards a femtosecond laser micromachined optofluidic device for distinguishing algae species," Proc. SPIE **7203** (2009).
20. F. He, Y. Cheng, L. Qiao, C. Wang, Z. Xu, K. Sugioka, K. Midorikawa, and J. Wu, "Two-photon fluorescence excitation with a microlens fabricated on the fused silica chip by femtosecond laser micromachining," Appl. Phys. Lett. **96**(4), 041108 (2010).
21. Scandinavian Culture Collection of Algae & Protozoa, "Z8," *http://www.sccap.dk/media/freshwater/7.asp*

1. Introduction

The early detection of algae proliferation is an important environmental issue as well as a public health issue since some algae can have noxious properties. The human health risk not only relates to drinking water but also recreational bathing water. For example, as a result of intensive human activities, the eutrophication of freshwater systems has favored the presence of cyanobacteria or "blue-green algae" that can produce potent toxins. Exposure to these compounds can result in acute poisonings that in some cases may be fatal [1]. At lower dosages, some cyanobacterial toxins are reportedly tumor promoters under some circumstances, if they are repeatedly taken in contaminated water [2]. Cyanobacterial toxins have been implicated in countless fatalities among domestic animals and have well-documented adverse ecological effects [3].

Presently, the assessment of the microbiological load in water requires that the specimen be transported to a laboratory after field-collection. Further individual tests for each micro-organism are cumbersome and must be performed by trained personnel. The delays with these steps reduce our ability to react effectively to an outbreak.

Consequently, there is a need for inexpensive monitoring methods that can characterize within a much shorter time period than current practice the threats posed by waterborne noxious organisms found in fresh or marine water. These devices should be operable by personnel with limited training. In this context, compact portable microfluidic–based instruments that can detect the presence of potentially noxious organisms in various water bodies are particularly attractive. Further, the interest in such devices goes beyond the identification of noxious organisms. More generally speaking, the identification of certain algal taxa and their quantities gives an indication of the water quality of river basins and bathing water. Note that new governmental regulations (like the ones issued by the European Commission [4]) direct civil authorities to carry out an effective algae load counting. Recently, with the quest for novel, cleaner and renewable energy, there has been a growing interest in using microalgae to create biofuels [5,6]. There, one foreseen challenge is to maintain oil-rich strands of algae from other competing species; to do so, some rapid methods to rapidly identify algae species are needed.

The recent development of femtosecond processing of fused silica [7–9] providing for the multifunctional integration of waveguides, fluidic channels [9] and micromechanical features [10] have opened exciting new avenues for the fabrication of compact and robust microorganism monitoring instruments [11]. In [12,13], we previously demonstrated the simultaneous fabrication of waveguides and fluidic channels and in [10] used this fabrication method to make a microdisplacement sensor. Others have fabricated related devices using femtosecond laser processing of substrates, primarily towards cell counting or sorting applications. These have included, in chronological order, a cell-sorting lab-on-a-chip [14], a

fluorescence detector added onto an existing chip [15], a single-cell detector [16], and an evanescent probe of a fluidic channel using fiber Bragg gratings [17].

This paper presents a new biochip concept and its application to the monitoring and classification of algae.

2. Biochip working principle

Previously we demonstrated a microdevice that counted particles flowing through a microfluidic channel [18]. This first generation device relied on a conceptually simple shadowgraphy implementation, where flowing particles briefly obstruct an external light source.

A salient feature of our second-generation device [19] is the integration of a curved sub-surface optical waveguide with a microfluidic channel in a monolithic fused silica substrate. The waveguide is used as a stable point-source that illuminates a small portion of fluidic channel. When objects (here algae) pass through the fluidic channel, the profile of the transmitted light is momentarily distorted. The light free-propagates after exiting the waveguide and, upon exiting the glass chip, is refocused towards a quadrant-cell detector that monitors very small intensity changes (Fig. 1).

The fluidic channel is formed by exposing the fused silica chip to the femtosecond laser, then etching the glass structure in a low-concentration HF bath. The fabrication of both waveguides and fluidic channels are further described in the next section.
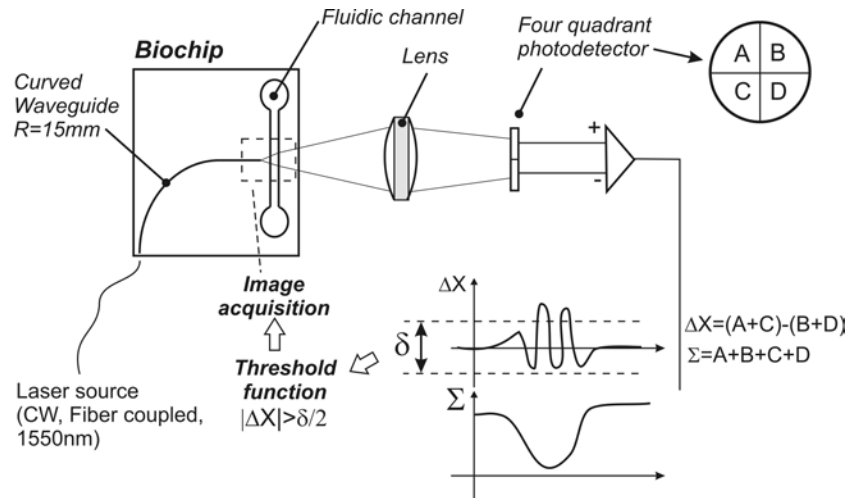

Fig. 1. Schematic of our biochip working principle: the biochip consists of a fluidic channel and a curved waveguide buried in the glass. A Gaussian beam emitted by a single mode fiber is coupled into the biochip waveguide and diverges to illuminate a small length of the fluidic channel. When objects pass through the fluidic channel, they momentarily distort the beam intensity profile. The light coming out of the biochips is then refocused onto a four-quad detector to monitor small changes of intensity.

3. Fabrication method and experimental setup

3.1. Biochip fabrication method

The bulk fused silica device comprises a straight microchannel with a curved waveguide with a 8 µm x 8 µm cross section; the waveguide is optimized to be single-mode at 1550 nm. To prevent uncoupled light from reaching the detector, the waveguide is 90-degree curved. The 18 mm radius of curvature is dictated by the delta n (a typical order of magnitude is 5×10^{-3}) of the waveguide. The waveguide ends perpendicular to a microchannel with a 100 µm x 100 µm cross section (see Fig. 1). The waveguide is fabricated in the bulk of the substrate (buried at a depth of 50 µm from the surface) using femtosecond laser pulses that locally increase the

refractive index of fused silica [7]. In the same laser-writing step, a volume region defining the microchannel is structurally modified at the surface of the chip. This region is later preferentially etched away in an HF bath to leave behind a surface with a trench removed (more details in Ref. [9]). A thick film made out of PDMS is used for sealing the channel. Fabricating the channel at the surface of the chip allows the fabrication of channels of arbitrary length, and the removable PDMS film permits the easy and thorough cleaning of the system between uses. Two hollowed cylinders (also made out of PDMS) are used as inlet and outlet. These fluidic interconnects are treated with oxygen plasma to form a robust permanent bond with the glass optofluidic device and to prevent leakage.
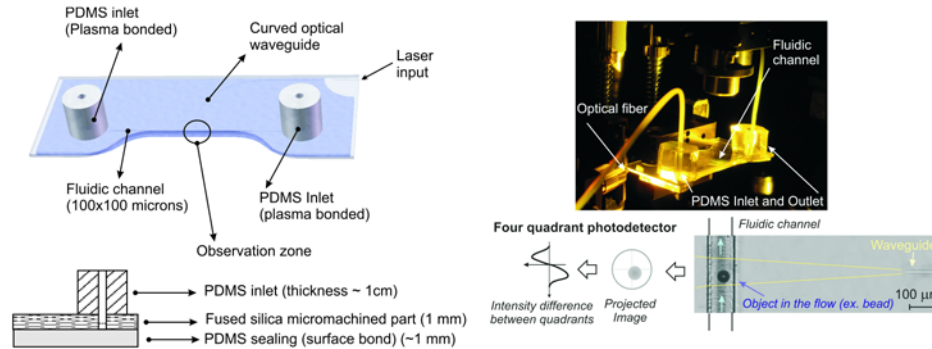
Fig. 2. (Left) General structure of the biochip. Top part: 3D CAD rendering, Bottom part: cross section of the biochips. The complete biochip is made of four parts: a glass part containing a fluidic channel and a buried waveguide, a PDMS layer sealing the top of the channel, and a PDMS inlet and outlet to allow fluidic connections. The optofluidic device has a curved subsurface waveguide which is femtosecond laser-formed in the fused silica substrate. (Right) The complete, assembled lab-on-a-chip is shown in the top image. The bottom image shows the waveguide and the fluidic channel with a bead passing by, with an outline of the measurement principle.

3.2. Experimental setup

The packaged optofluidic device, shown in Fig. 2, is interfaced with a syringe pump and a reservoir. To illuminate the fluidic channel locally, a fiber-coupled infrared laser source (1550 nm, 2.5 mW from Thorlabs S1FC1550) is aligned at the beginning of the waveguide. The beam diverges slowly after exiting the waveguide and illuminates the full height of a small section of the channel; the very low numerical aperture of the waveguide – typically around 0.12 – makes the beam quasi-collimated. In order to detect and identify components as they flow past the waveguide, a quadrant-cell photoreceiver (New Focus 2903) is placed on the optical axis where the curved waveguide ends to measure the transmitted light. A lens (illustrated in Fig. 1) is used to focus the beam emerging from the waveguide so that it covers the entire active area of the sensor (3 mm x 3 mm). This lens, and possibly other optical components, could eventually be integrated into the system with the same femtosecond laser fabrication process in a manner similar to that demonstrated in [20]. The sum signal from all four quadrants of the photoreceiver is constantly monitored at 2 kHz, and a second signal simultaneously measures the difference between the summed upstream cells and the summed downstream cells (Σ and ΔX in Fig. 1, respectively).

To evaluate the detection and identification performance of the optofluidic device, a high-speed camera (AVT PIKE F-032B) is used to image specimens as they flow past the waveguide (Fig. 3). This camera analysis only serves the purpose of correlating the library of collected signals with the objects passing in the fluidic channels. It allows us to cross-check collected information and to build up a database of signals. This database can then be used to identify the signal shapes obtained from the device without the camera.

If the difference signal from the photodetector rises above a user-defined threshold ($|\Delta X| > \delta/2$, as in Fig. 1), a signal is sent to the camera to trigger the acquisition of an image,

such as those shown in Fig. 3, and the photodetector signals are recorded. A real-time Simulink model is used to control the data acquisition and to trigger the high-speed image acquisition system operating at 120 fps when an alga or other particle is detected. The trigger and quad-cell signals are recorded with the same reference time, allowing us to accurately correlate the measured signal with the corresponding image and therefore to identify the algae. Only a small number of points are recorded when an event is detected. This way, long-lasting experiments can be done without the need for extensive computer memory.

When an alga transits through the analytical beam, the quadrant-cell detector sum signal shows an attenuation, and the difference signals reveal distinct wavelet-like signals, such as those seen in Fig. 3. These signals offer a qualitative means of distinguishing the various algae types. The distinct nature of the wavelets is related to the particular geometry, and associated optical properties, of the algae. If the cell is not axially symmetric and/or happens to be rotating as it flows past the waveguide the wavelet centro-symmetry is broken.

Experimental data were collected with five species of algae: one cyanobacterium (*Cyanothece)*, three species of green algae (*Monoraphidium*, *Scenedesmus*, *Nephrochlamys*) and one species belonging to the family of Desmidiaceae (*Staurastrum*). The algae were selected to represent different taxonomic groups, sharing a similar size, while differing in geometry. The species coexist in nature and co-occur in many environmental samples. Algal cultures were provided by the Norwegian Institute for Water Research Culture Collection of Algae and were kept in Z8 culture medium [21]. The flow rate in the microfluidic channel was on the order of 2-3 µL/min, resulting in an average in-channel water velocity of 3-5 mm/s.
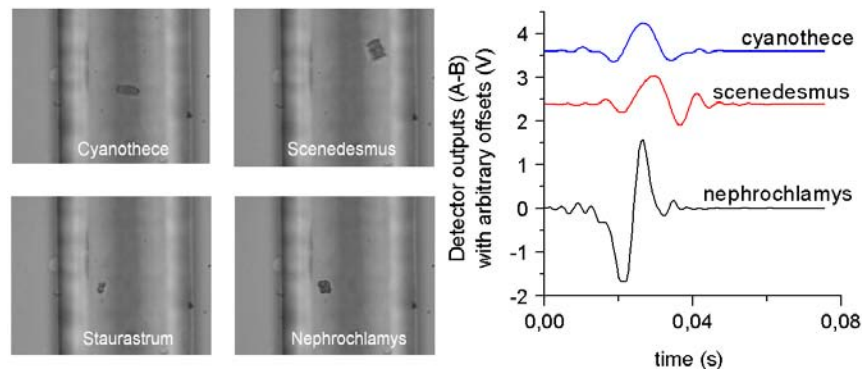

Fig. 3. Images (left) taken on the fly by the camera (with a 20X objective) overlooking the fluidic channel. Image capture is triggered by the sample signals (right) rising above a set threshold. The channel width is 100 microns. Algae as small as 10-20 microns can be detected using this technique. Note the very low signal-to-noise ratio.

4. Results and discussions

To correlate the photodetector signals with the algae species, a convolution algorithm was prepared to quantitatively compare photodetector signals (Fig. 3) with a set of test functions (Fig. 4). Three shapes were chosen for the test functions ($i = 1,2,3$) and each was scaled to four lengths in the time domain ($j = 1,2,3,4$); these shapes were taken directly from representative signals from the algae samples, and the time scales were chosen based on the range of signals observed in the data.

Each photodetector signal recorded from an algae incident was normalized so the signal in the first 10 ms of the test had an average of zero, and so that the maximum value of the signal was 1. Each of the twelve test shapes f_{ij} were convolved against each of the normalized photodetector signals $h_k(t)$ for a collection of n data sets ($1<k<n$). The convolution result

$$c_{ijk} = f_{ij} * h_k (t) \tag{1}$$

was produced for each combination of i, j, and k. Next, the maxima

$$m_{ik} = \max(c_{ijk})$$ (2)

were found, so that m_{ik} represents the maximum value found in the convolution outputs for test k with any shape in the set i. Thus, for any test k there are three values of m_{ik}, representing how well that test k matched with the set i (*i.e.*, with the shapes in Fig. 4).
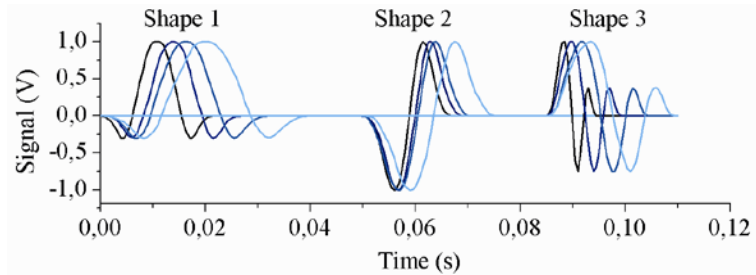

Fig. 4. The three test function shapes f_{ij} used in the convolution process, with an arbitrary position in the time axis. Each shape is a set of four sub-shapes, each scaled differently in time, shown with progressively lighter shades.

Figure 5 shows the correlation results for 619 data sets. The *Cyanothece* showed a strong correlation with the test function "Shape 1", and were distinguishable from the four other species by their strong correlation with this function and their limited correlation with the other functions (Fig. 5).

Based on these results, three conditions based on the range and ratios of the m_{ik} values were imposed to distinguish the *Cyanothece* algae from the other species:

$$10 < m_{1k} < 22$$

$$1.1 < \frac{m_{2k}}{\sqrt{m_{1k}}} < 4$$ (3)

$$2.5 < \frac{m_{3k}}{\sqrt{m_{1k}}} < 4$$

If an experiment's m_{ik} values satisfied all three requirements, the algae was classified as *Cyanothece*. These values were chosen to balance a high ratio of positive detection with a low ratio of false positives; in this manner, 93% of the 216 *Cyanothece* algae were positively identified, while 8% of the 403 other algae occurrences were falsely identified as *Cyanothece*.
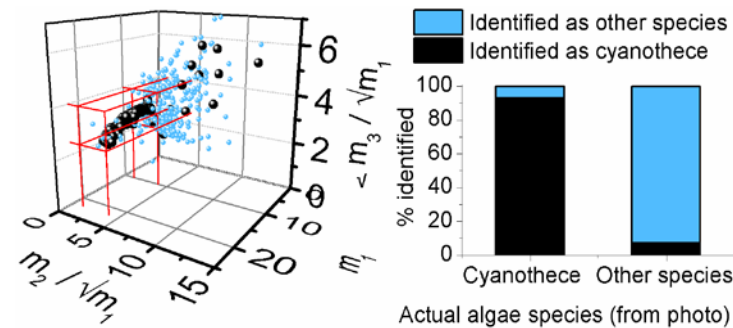

Fig. 5. (Left) The m_i values for each test, representing the maximum value found in the convolution of the test with the sets of test function shapes shown in Fig. 4. The black points are *Cyanothece* (216 tests), as identified visually from the microscope photos, and the lighter blue points are all other species (403 tests). The volume in m-space chosen as in Eq. (3) to distinguish the *Cyanothece* is marked in red . (Right) Summary of the results of the automated method for distinguishing *Cyanothece* from the other algae species.

5. Conclusion

We have fabricated a functioning compact femtosecond laser-machined optofluidic device that can detect, monitor, and qualitatively distinguish algae species free flowing in a water stream. Using a quadrant-cell photoreceiver, we have shown that algae generate distinctive wavelets that can be associated with the particular algae geometry. These results demonstrate that even a single waveguide instrument can provide a basic algae identification function. Adding another waveguide, we expect to extract more quantitative information such as accurate algae size, precise flow rate, etc. Other areas for future development include a more compact flow-handling system to replace the current syringe pump, and the addition of geometrical features or other sensing technologies which will allow the system to overcome challenges which may arise from irregularly shaped or arbitrarily oriented algal samples.

Our field-compatible compact optofluidic device will provide most of the information available from more complex image-based systems. Furthermore, the approach based on integrated optics has the potential to provide additional information including specific optical properties such as algal fluorescent response, which can be used to further identify the algae.

The optofluidic device has important characteristics which are made possible when fused-silica is micromachined with femtosecond laser. The single-mode curved waveguide yields robust detection results particularly when difference signals are used. Thanks to the flexibility of the manufacturing process, the microchannel size and shape can be adapted to a variety of problems. Furthermore, the vicinity of the waveguide to the channel can be tuned to control the portion of the channel height that is illuminated to optimize detection or study refractive properties. The exclusive use of free-space optics involved in the setup, and the fact that a laser diode source and quad-cells could be packaged with the device, open interesting prospects for field-based pathogen detection devices.